XLIII CILAMCE
21-25, November, 2022
FOZ DO IGUAÇU – PR – BRAZIL

Analysis of global stability of guyed towers considering unilateral constraints

Fernanda Neves da Silva[1], Frederico Martins Alves da Silva[1]

[1]*School of Civil Engineering, Federal University of Goiás, UFG*
Av. Universitária, n.º 1488 - quadra 86 - Setor Leste Universitário, 74605-010, Goiânia, Goiás, Brasil
fernanda_neves@discente.ufg.br, silvafma@eec.ufg.br

Abstract. Guyed structural systems are present in several engineering applications, and as a large portion of these structures have a high level of slenderness, their designs are based on stability criteria. The set of cables present in these elements are characterized by high efficiency when they are tensioned. The main objective of this study is to analyze the static and dynamic nonlinear behavior of a discrete guyed tower model with two degrees of freedom. Furthermore, the present work devotes special attention to the consideration of the unilateral contact (boundary condition) in the nonlinear oscillations of this structure. The unilateral contact is manifested in this type of application from the consideration of the capacity of the stays to resist only the traction efforts, as an effect, this approach strongly modifies the analysis of the proposed structural system. For this model, there is a significant influence of the consideration of unilateral contact on the post-critical behavior, with a marked decrease in the critical load of the structure. Thus, the results show that this type of structure is highly sensitive to geometric nonlinearities and to the restriction of certain stays, indicating that these effects must be considered in the tower design phase.

Keywords: Guyed towers, Unilateral constraints, Non-linear static analysis, Nonlinear dynamic analysis.

1 Introduction

The improvement of construction techniques, associated with the use of new materials and the development of new technologies, has resulted in projects of increasingly slender, light and flexible structures. Guyed structural systems contain these aspects and are widely used in many engineering applications. As the structural elements are designed with greater slenderness, the structure becomes more susceptible to lateral deflections. Thus, as evidenced by Del Prado *et al*. [1], geometric nonlinearities are associated with their static and dynamic behavior. Carvalho [2] reports that the efficiency of cable-stayed structures to support axial loads is due to the presence of cable elements, which present high efficiency when subjected to traction, fully meeting the architectural and structural concepts required.

Marques *et. al* [3] investigate the influence of cable configuration on the static and dynamic stability of guyed towers through a nonlinear finite element model. The results show that guyed towers have a highly non-linear response, even at low load levels. In addition, the uniform distribution of cables can give rise to coincident buckling loads and vibration frequencies.

Given the importance of cable analysis, Sequeira *et. al* [4] report that many accidents occur in guyed towers due to cable rupture. Thus, the authors investigate the sudden rupture of one or two cables, arbitrarily selected, in the linear and non-linear response of the guyed tower under static and dynamic loads of a tower model studied via finite elements. The results show that this type of structure is sensitive to physical and geometric nonlinearities and to rupture, indicating that these should be considered in the design of the tower structure. This research shows that cable failure produces a reduction in buckling load and vibration.

According to Barbosa [5], some structures may be in unilateral contact, which are boundary conditions that resist the displacements of bodies only in certain directions or prevent such displacements. In this context, it can be said that guyed towers are a class of structures in which the consideration of the hypothesis of unilateral contact of the cables - which resist the displacements of the tower if tensioned - must be considered to obtain a more accurate mathematical model.

In this sense, this work intends to investigate the unilateral contact (boundary condition) in the non-linear oscillations of guyed towers. The unilateral contact is manifested in this type of application from the consideration of the capacity of the structure cables resist only the traction forces, which strongly modifies the static and dynamic analysis of the proposed structural system. From this contextualization, the analysis of stability and non-linear vibrations of guyed towers is carried out, considering the unilateral contact of cables in the equivalent mathematical model.

2 Mathematical formulation

The plan tower discrete model studied consists of a central mast comprising two labeled rigid bars. The lower bar of length h_1 has a rotational spring at its lower end, and a spring at the upper end that connects it to a consecutive rigid bar of length h_2. The lateral displacements are restricted by translational linear springs corresponding to the cables, responsible for ensuring the stability of the structure. These springs with stiffness coefficients k_1, k_2, k_3 and k_4 are fixed at anchor points arranged at a distance L from the tower and at the ends of each rigid bar.

The tower is subjected to three loads, being an axial load P, applied at its end, and axial loads p_1 and p_2, corresponding to the self-weight of the bars of length h_1 and h_2, respectively. The system has two rotational degrees of freedom denoted by θ_1 and θ_2, angles that represent the rotations associated with rotational springs with stiffness coefficients $k_{\theta 1}$ and $k_{\theta 2}$, respectively. Therefore, each bar has a unique degree of mobility, and the structure is characterized by the series of these two variables that uniquely determine its position. In Fig. 1(a), the tower is shown in the fundamental equilibrium configuration, and in Fig. 1(b), the deformed configuration of the structure.

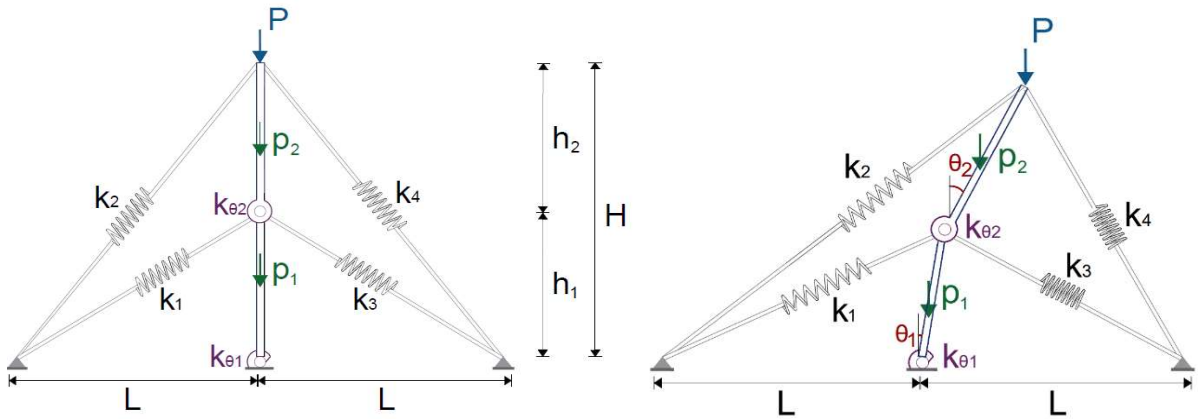

(a) initial configuration (b) deformed configuration

Figure 1. Geometric model in (a) initial and (b) deformed configuration.

The study of stability based on the energy criterion relates the internal energy of deformation and the work done by the external forces of the structure. The variation of the spring length, Δl_{i}, is expressed by the sum of an initial elongation Δl_0, caused by the prestressing force acting on the cables, plus the elongation Δl_P, as a function of the rotations of the bars when they undergo the action of external stresses. Then Δl_{i} is written in the form:

$$\Delta l_i = (\Delta l_0)_i + (\Delta l_P)_i, \tag{1}$$

where the elongation due to the prestressing of the stays is given by:

$$(\Delta l_0)_i = -(F_0)_i \,/\, k_i. \tag{2}$$

It is noteworthy that the angles θ_1 and θ_2 are considered positive in the direction of rotation indicated by Fig. 1(b). The expressions of Δl_P when calculating the variation between the final and initial lengths of the four analyzed springs, considering the proposed rotation direction, are given by:

$$\begin{aligned}
\Delta l_{p_1} &= \sqrt{h_1^2 + 2\,L\,h_1\,sin\,\theta_1 + L^2} - \sqrt{h_1^2 + L^2}\,, \quad \Delta l_{p_3} = \sqrt{h_1^2 - 2\,L\,h_1\,sin\,\theta_1 + L^2} - \sqrt{h_1^2 + L^2}, \\
\Delta l_{p_2} &= \sqrt{h_1^2 + h_2^2 + 2\,h_1\,h_2\,cos(\,\theta_2 - \theta_1) + \,2\,L\,(h_2\,sin\,\theta_2 + \,h_1\,sin\,\theta_1) + L^2} - \sqrt{H^2 + L^2}, \\
\Delta l_{p_4} &= \sqrt{h_1^2 + h_2^2 + 2\,h_1\,h_2\,cos(\,\theta_2 - \theta_1) - \,2\,L\,(h_2\,sin\,\theta_2 + \,h_1\,sin\,\theta_1) + L^2} - \sqrt{H^2 + L^2}.
\end{aligned} \tag{3}$$

The internal deformation energy of the system considers the contributions of the energy referring to each translational spring, and the related rotational springs. The work of external loads considers the effects of loads P, p_1 and p_2 applied to the structure. So, the sum of these energies results in the variation of the total potential energy:

$$\begin{aligned}
\Delta\pi = \frac{1}{2}\sum_{i=1}^{4} FS_i\,k_i\,(\Delta l_{0i} + \Delta l_{pi})^2 + \frac{1}{2}\,k_{\theta 1}\,\theta_1^2 \, + \frac{1}{2}\,k_{\theta 2}\,(\theta_2 - \theta_1)^2 - P\,(H - h_1\,cos\,\theta_1 - h_2\,cos\,\theta_2) \\
- p_1\left(\frac{h_1}{2} - \frac{h_1\,cos\,\theta_1}{2}\right) - p_2\left(H - \frac{h_2}{2} - h_1\,cos\,\theta_1 - \frac{h_2\,cos\,\theta_2}{2}\right),
\end{aligned} \tag{4}$$

where the parameter FS_i represents the *Signum* function, responsible for introducing in this formulation the consideration of unilateral contact. This function is a mathematical consideration that extracts the sign of a real or complex number and, when applied to the terms of the internal deformation energy referring to the cables, fulfills the objective of disregarding such elements subjected to compression. In this context, to perform an analysis that meets the unilateral contact, FS_i must assume the following expressions:

$$FS_{\mathrm{i}} = \left(\frac{signum\,\Delta l_{p_i}}{2} + \frac{1}{2}\right), i = 1, 2, 3, 4. \tag{5}$$

However, for an analysis that does not consider this restriction promoted by unilateral contact, that is, the effects of all cables will be accounted for in the study of the behavior of the structural system (bilateral contact), FS_i must assume a unit value.

The system of nonlinear equilibrium equations of the post-critical path is obtained by deriving the expression of the total potential energy, indicated by Eq. (4), as a function of the generalized coordinates, θ_1 and θ_2:

$$\begin{aligned}
&\frac{1}{2}\sum_{i=1}^{4}\frac{d}{d\theta_1}\left(\,FS_i\,k_i\,(\Delta l_{0i} + \Delta l_{pi})^2\right) - \frac{p_1\,h_1\,sin\,\theta_1}{2} - p_2\,h_1\,sin\,\theta_1 + \,k_{\theta 1}\,\theta_1 - \,k_{\theta 2}\,(\theta_2 - \theta_1) \\
&\qquad - P\,h_1\,sin\,\theta_1 = 0, \\
&\frac{1}{2}\sum_{i=1}^{4}\frac{d}{d\theta_2}\left(\,FS_i\,k_i\,(\Delta l_{0i} + \Delta l_{pi})^2\right) - \frac{p_2 h_2\,sin\,\theta_2}{2} + k_{\theta 2}\,(\theta_2 - \theta_1) - P\,h_2\,sin\,\theta_2 = 0.
\end{aligned} \tag{6}$$

The equilibrium path of the system, after passing to the post-critical path, is determined using the standard Newton-Raphson method. At the end of the following iterations, there is a series of values for P, θ_1 and θ_2 that configure the non-linear equilibrium trajectory, thus allowing the visualization of the different post-critical paths when plotting those points.

The equation of motion can be determined from the Lagrangian approach, which involves the kinetic energy T and the total potential energy Π. Obtaining the kinetic energy, that comprises two rigid bars with the density of the material, ρ, and that the cross-sectional area, A, the equations of motion have associated dynamic properties and are given by:

$$\frac{\rho\,A\,h_1^3}{3}\,\ddot{\theta}_1 + c\,\dot{\theta}_1 + \frac{d\Delta\Pi}{d\theta_1} = 0 \quad \text{and} \quad \frac{\rho\,A\,h_2^3}{3}\,\ddot{\theta}_2 + c\,\dot{\theta}_2 + \frac{d\Delta\Pi}{d\theta_2} = 0. \tag{7}$$

The second order differential equations set, Eq. (7), are transformed into systems of first order differential equations of motion. Then these systems are integrated in time using the 4-th Runge-Kutta method. It is important to notice that from the set of first order differential equations of motion, a Jacobian matrix can be obtained. The

classification of equilibrium points is determined by the eigenvalues λ_1, λ_2, λ_3 and λ_4 of the Jacobian matrix. Ricardo [6] approaches the classification of the stability of fixed points from the numerical characteristic of λ_i. According to the author, if all the eigenvalues have the real parts equal to zero, and the imaginary parts are not zero, there is a stable center. If all the reals are negative, the point is stable, if at least one eigenvalue has a positive real part, it is classified as unstable. A node and a focus are different equilibrium points where the first one all imaginaries must be null while the focus has its imaginary part not null. The saddle is characterized by having real eigenvalues with opposite signs.

3 Numerical results

To obtain the static numerical results, the following values corresponding to the parameters involving the were considered: $h_1 = h_2 = 3.5\ m, H = 7\ m, L = 4\ m, p_1 = p_2 = 0.14\ N, k = 1\ N/m, F_0 = 0.01\ N, k_{\theta 1} = 1\ N/rad$ and $k_{\theta 2} = 0.5\ N/rad$.

Figure 2 shows the nonlinear equilibrium path of the structural system under bilateral contact, projected in the two orthogonal planes, $P \times \theta_1$ and $P \times \theta_2$. The continuous lines correspond to the stable equilibrium configurations and the dashed lines to the unstable configuration.

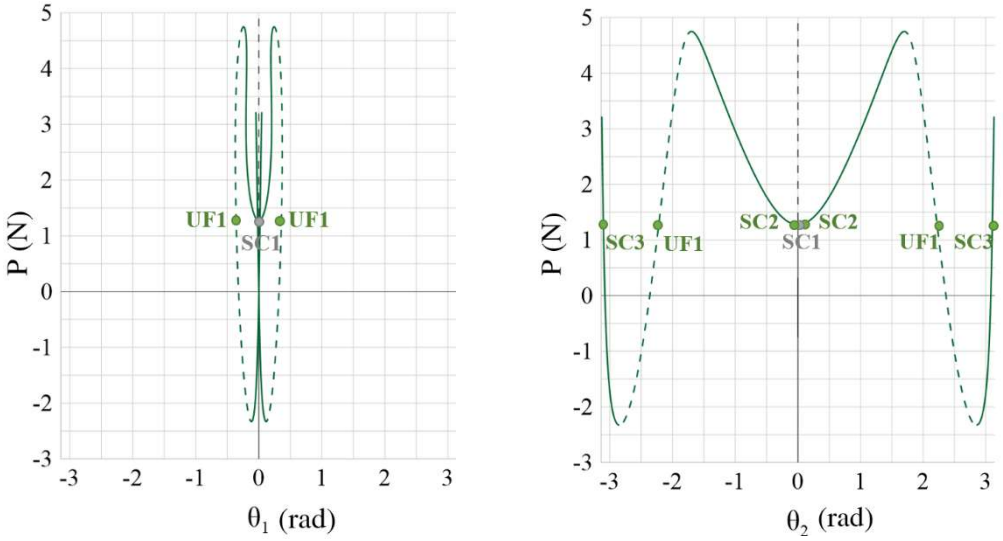

(a) in the P × θ_1 plane

(b) in the P × θ_2 plane

Figure 2. Post-critical path of the discrete model that considers bilateral contact (a) in the P × θ_1 plane (b) in the plane P × θ_2.

As the compressive load increases, a stable nonlinear path with increasing effective stiffness up to the first maximum limit point ($P_{lim} = 4{,}74$ N) is observed. The limit point is followed by a significant decrease in stiffness to a minimum point, and from there, the stiffness increases again. Thus, it appears that the post-critical path is comprised of two paths in which the symmetric bifurcation is stable, the interval of the first path is given by $0° < \theta_1 < 13.9°$ and $0° < \theta_2 < 97.4°$, and the other section is stable at $2.4° < \theta_1 < 6.4°$ and $163.8° < \theta_2 < 180°$. The corresponding symmetrical intervals, which have the same negative angulations, are also stable.

The post-critical paths shown in Fig. 3 are obtained by considering unilateral contact for these same study parameters. Analogously to the post-critical path obtained for the bilateral contact, it is noted that the nonlinear equilibrium paths along the displacements are symmetrical. However, in this case there is no presence of critical bifurcation load, therefore, there is no fundamental path of equilibrium. In the absence of a critical load, the limit point load ($P_{lim} = 0.60\ N$), associated with rotations θ_1 and θ_2 very close to zero, is analyzed. It is noteworthy that P_{lim} is lower than the critical load obtained in the analysis of the system with bilateral contact, given by $P_{cr} = 1.28$ N. Therefore, when considering the unilateral contact for this same case, it appears that there is a considerable loss of rigidity of the structural system. A stable path with increasing effective stiffness is observed for small rotations, until the system reaches the point of P_{lim}. It is verified that the trajectory are stable in the path composed

by the intervals of $0.35° < \theta_1 < 1.35°$ and $1.14° < \theta_2 < 4.01°$, and in the other path varying between $-3.43° < \theta_1 < 31.03°$ and $74.48° < \theta_2 < 158.14°$. When comparing the trajectories presented for the two forms of contact shown by Figs. 2 and 3, it is noticeable that the stable paths do not comprise precisely the same interval in both cases, since few stable intervals correspond. For unilateral contact, there is a greater restriction for displacements related to θ_2 compared to the other form of contact. On the other hand, there are larger intervals of stable θ_1 in the case where unilateral contact is considered.

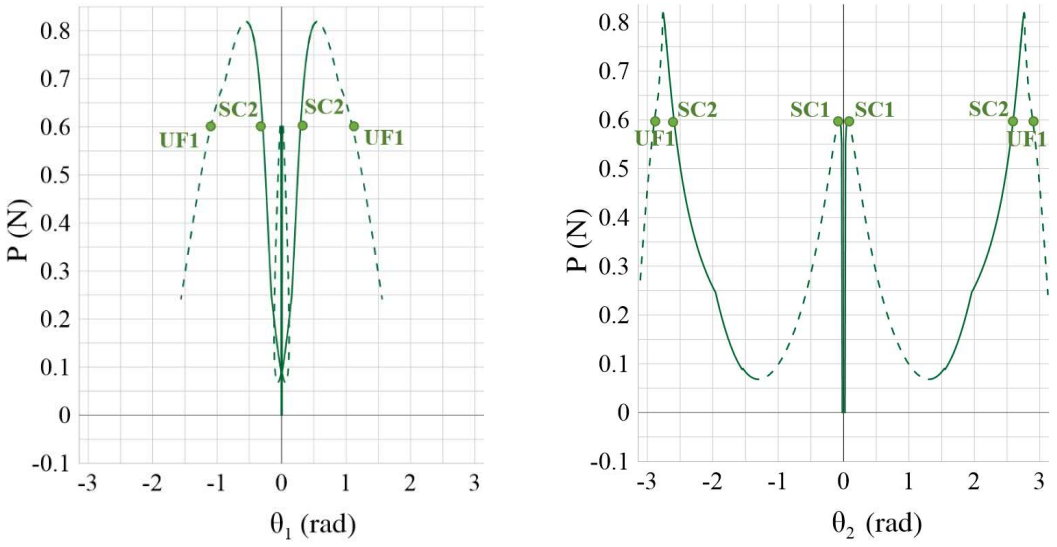

(a) in the $P \times \theta_1$ plane (b) in the $P \times \theta_2$ plane

Figure 3. Post-critical path of the discrete model that considers unilateral contact (a) in the P × θ_1 plane (b) in the plane P × θ_2.

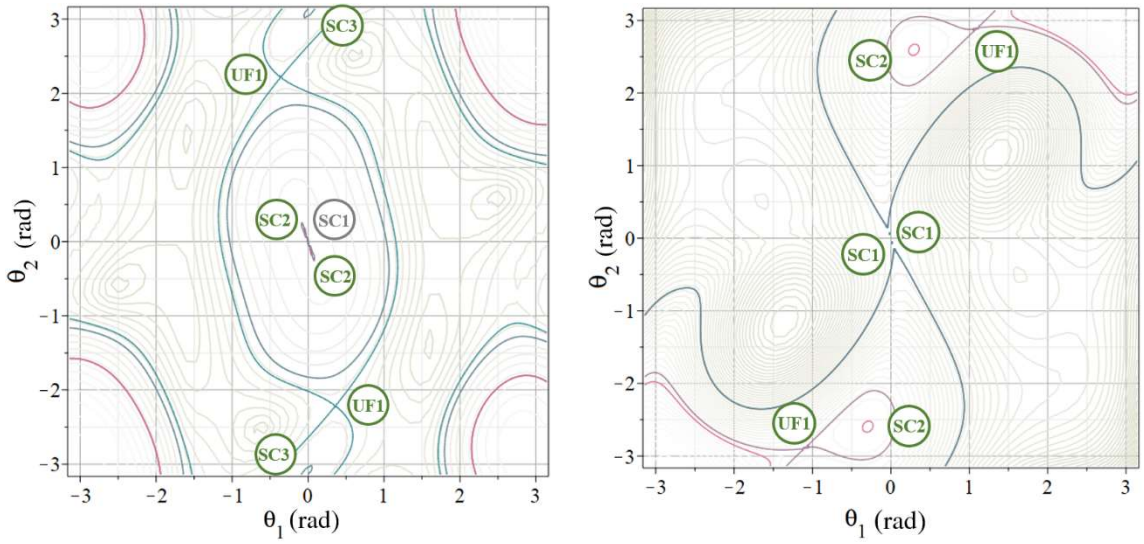

(a) bilateral contact (b) unilateral contact

Figure 4. Potential energy surface curves considering (a) bilateral contact and (b) unilateral contact.

A clear understanding of the structure's nonlinear behavior can be observed in the surfaces of the structure's total potential energy for chosen load levels. For this analysis, the load parameters $P = P_{cr}$ and $P = P_{lim}$were adopted to classify all static equilibrium points along the nonlinear equilibrium trajectories referring to the case of bilateral and unilateral contact, respectively. Notable points have been indicated in Figs. 2 and 3, as well as in the isocurves of the total potential energy of the bilateral and unilateral contact cases, as shown in Fig. 4. Note that the

total potential energy curves, that consider the bilateral contact (Fig. 4(a)) have seven configurations of static equilibrium: a minimum corresponding to the stable equilibrium position along the fundamental trajectory (SC1 – Stable Center 1), two unstable equilibrium positions along the trajectory (UF1 – Unstable Focus 1), and four stable equilibrium positions (SC2 and SC3 – Stable Centers 2 and Stable Centers 3). Symmetric points are designated with the same nomenclature, as there is no differentiation between their coordinates. On the other hand, for the consideration of unilateral contact, Fig. 4(b) shows the existence of six static equilibrium configurations for the analyzed load: two centers corresponding to stable equilibrium positions under small displacements (SC1), two foci related to unstable equilibrium positions along the trajectory (UF1), and two centers related to stable equilibrium positions with large displacements of θ_2 (SC2). The classification of these points was obtained on the analysis of the stability study according to Lyapunov. From Fig. 4, it was observed important changes in the topology of the total potential energy due to the nonlinearity inserted by the signum function, leading to a complex behavior competition between the potential wells.

For plan tower discrete model subjected to the harmonic force, the evolution of the time response of the θ_1 and θ_2 rotation of the tower when subjected to harmonic axial loading in the form $P = F_1 + F_2\, cos(\Omega t)$ is analyzed. F_1 and F_2 are ratios of critical load, and Ω is equal to the pre-loaded structure's natural frequency, which in this case is $\Omega = 0.258\, rad/s$. In addition, were adopted: $c = 0.01, A = 0.1\, m^2$ e $\rho = 0.01\, kg/m^3$.

The equations of motion, Eq. (7), are time-integrated for different values of F_2 starting from small values of θ_1 and θ_2. F_1 was considered equal to $0.75\, P_{cr}$. Figure 5 shows some time responses and phase portrait for the model with bilateral contact hypothesis of guyed cables. It can be seen in Fig. 5(a) the presence of small disturbances with the permanent response going to the fundamental solution, that is, after a harmonic load perturbation, the amplitude of the response rapidly decreases, converging to the trivial solution. When increasing the value of F_2, as seen in Fig. 5(b), the maximum amplitude of the response will increase, experiencing a periodic stable orbit inside the potential well with stable centers SC1 and SC2. The permanent response of this system is characterized by phase portrait plane of Fig. 5(c).

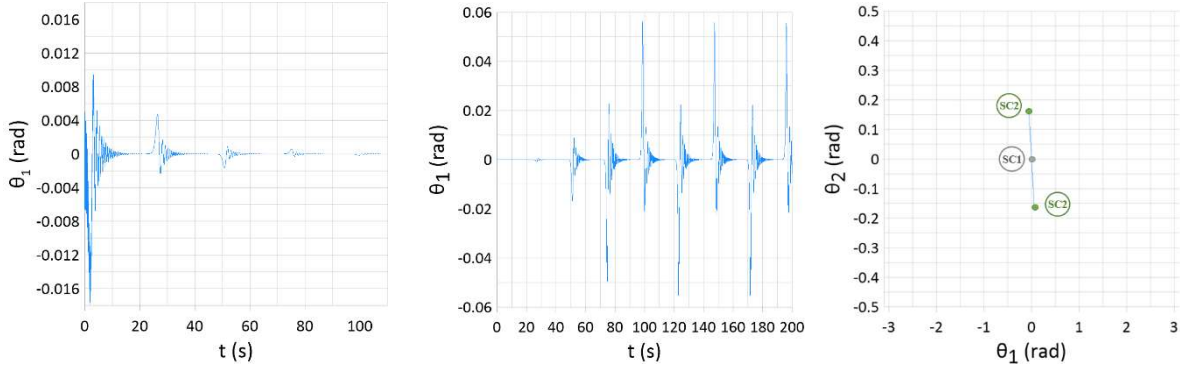

(a) $F_2 = 0.22\, P_{cr}$ (b) $F_2 = 0.25\, P_{cr}$ (c) Phase plane for $F_2 = 0.25\, P_{cr}$

Figure 5. Time response and phase plane of the discrete model under bilateral contact according to variation in F_2.

Regarding the system that considers unilateral contact of guyed cables, the evolution of the response over time was also analyzed by varying the values corresponding to the F_2. In Fig. 6(a) it is evident that, after an initial harmonic load perturbation, the response amplitude decreases converging to a periodic stable solution around to the potential well around SC1 point. However, when adopting $F_2 = 0.25\, P_{lim}$, as indicated in Fig. 6(b), large-amplitude vibrations are observed, and an initial cross-well motion occurs leading the system to oscillate in the steady-state around the SC2 potential well. The phase portrait plans corresponding to the solutions obtained in Fig. 6(a) and Fig. 6(b) are indicated in Fig. 6(c).

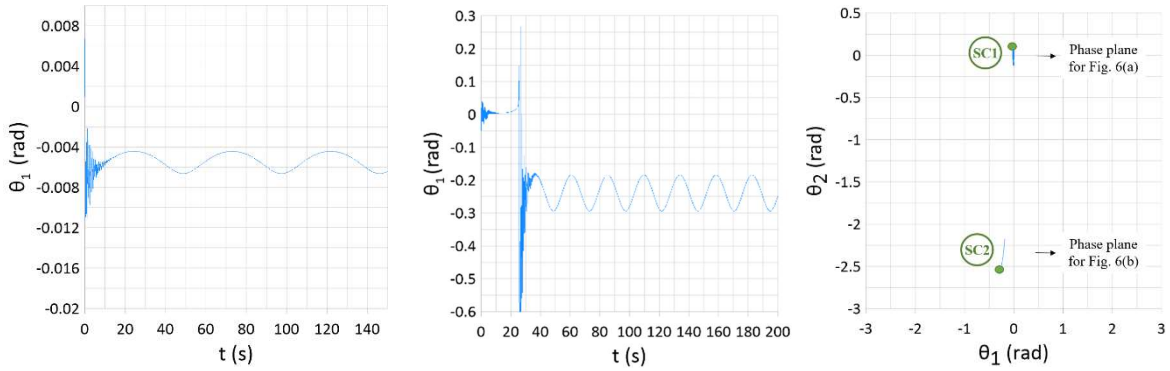

(a) $F_2 = 0.10\ P_{lim}$ (b) $F_2 = 0.25\ P_{lim}$ (c) Phase plane

Figure 6. Time response and phase plane of the discrete model under unilateral contact according to variation in F_2.

4 Conclusions

A mathematical discrete model capable of considering only the cables that are effectively tensioned was developed for a plan guyed tower discrete system. The presence of static loads and, mainly, dynamic loads in nonlinear structural systems, such as the investigated tower model, are factors that make a meticulous analysis of the behavior of these structures necessary. As evidenced in the static and dynamic results, the consideration of unilateral contact in the analysis of the stability of the structural system is responsible for strongly changes in the nonlinear equilibrium responses, since there is a considerable loss of rigidity of the structural system. In the analysis of the non-autonomous system, a relationship between the total potential energy and the phase portrait was used, where it is observed that the system initially oscillates around a post-critical equilibrium configuration and, when the load amplitude varies starts to oscillate around another potential well equilibrium position. This work is under development, evaluating the global nonlinear dynamic behavior from an extensive parametric analysis of the harmonic load.

Acknowledgements. This work was made possible by the support of the Brazilian research agency CNPq, CAPES and FAPEG (Fundação de Apoio e Amparo à Pesquisa do Estado de Goiás).

Authorship statement. The authors hereby confirm that they are the sole liable persons responsible for the authorship of this work, and that all material that has been herein included as part of the present paper is either the property (and authorship) of the authors, or has the permission of the owners to be included here.

References

[1] Z. J. Del Prado, E. C. Carvalho, P. B. Gonçalves, "*Dynamic stability of imperfect cable stayed masts*". Mecánica Computacional, Argentina, vol. 29, n. 7, pp. 647-658, 2010.
[2] E. C. Carvalho. *Análise da Instabilidade Dinâmica de Estruturas Estaiadas*. Master's thesis, Universidade Federal de Goiás, 2008.
[3] Í. R. Marques, P. B. Gonçalves, D. M. Roehl, "Effect of the cable system on the static and dynamic stability of Guyed Towers". *III Pan-American Congress on Computational Mechanics*, 2021.
[4] L. E. F. Sequeira, P. B. Gonçalves, D. M. Roehl, "Influence of Guy Rupture and Plasticity on the response of Guyed Telecommunication Towers". *III Pan-American Congress on Computational Mechanics*, 2021.
[5] H. J. C. Barbosa. *Algoritmos numéricos para problemas de contato em elasticidade*. PhD thesis, Universidade Federal do Rio de Janeiro, Rio de Janeiro, 1986.
[6] H. J. Ricardo. *A Modern Introduction to Differential Equations*. Elsevier, 2009.